PROCEEDINGS OF SPIE

SPIEDigitalLibrary.org/conference-proceedings-of-spie

Testing novel miniature NIR spectrometers for wearable broadband NIRS devices

M. Talati, F. Lange, I. Tachtsidis

M. Talati, F. Lange, I. Tachtsidis, "Testing novel miniature NIR spectrometers for wearable broadband NIRS devices," Proc. SPIE 12628, Diffuse Optical Spectroscopy and Imaging IX, 126282B (9 August 2023); doi: 10.1117/12.2668162

SPIE.

Event: European Conferences on Biomedical Optics, 2023, Munich, Germany

Testing novel miniature NIR spectrometers for wearable broadband NIRS devices

M. Talati*[a], F. Lange[a], I. Tachtsidis[a]
[a]Department of Medical Physics and Biomedical Engineering, University College London, Malet Place Engineering Building, Gower Street, London WC1E 6BT, UK
*musa.talati.20@ucl.ac.uk

ABSTRACT

The feasibility of new-generation miniature spectrometers for use in portable broadband NIRS (bNIRS) devices was explored in this investigation. The study outlines tests of varying integration time between 1000 ms, 500 ms and 250 ms and source-detector separations between 2 cm, 3cm and 4 cm, and their effect on the received signal through MEDPHOT tissue-mimicking phantoms, A2, B2, B3 and D7, using the Oceans Optics HL-2000-HP tungsten halogen lamp as a broadband light source. The spectra and SNR were then compared to two gold-standard bNIRS systems. It is found that two of the spectrometers give respectable SNR values for the detection range of 600 - 1000 nm in all regimes except when saturated or using phantom D7. It is demonstrated that these two devices can appropriately be used for source-detector separations of 3 cm and 4 cm at 500 ms and 1000 ms integration times, to determine absorption changes in tissue and thus chromophore concentrations. To use them for 2 cm separations, an additional attenuation component will be required.

Keywords: Broadband NIRS, Spectrometer, Signal-to-noise ratio, integration time, source-detector separation

1. INTRODUCTION

Near-infrared spectroscopy (NIRS) is a non-invasive imaging technique which can be used to monitor the changes in blood oxygenation and cellular metabolism by guiding NIR light, wavelengths of 650-1000 nm, through tissue and measuring the reflected light intensity. Functional NIRS (fNIRS) has been proven to be a highly valuable tool for monitoring cerebral development in a wide range of environments[1]. Although, current commercial implementations only provide cerebral oxygenation measurements and have limited ability in measuring the metabolic changes that are important for neurodevelopment assessments[2]. Broadband NIRS (bNIRS) is an extension of fNIRS that provides the same assessment of cerebral oxygenation biomarkers, along with a valuable marker for oxygen metabolism at a cellular level, the oxidation state of cytochrome-c-oxidase (oxCCO). The challenge in resolving the oxCCO signal in-vivo lies in its significantly smaller concentration compared to the haemoglobin, at around a tenth[3]. bNIRS implements many, often in the hundreds, of wavelengths in the full NIR spectrum to address this and provide insight to tissue energetics. To supply these many wavelengths of light, broadband sources are required, and spectrometers are employed to distinguish the power per wavelength after reflection. Current multi-channel bNIRS instruments are bulky and only semi-portable, requiring significant effort to move from room to room, due to the technological limitations. There is an urgent need to bring these up to the state of fNIRS systems, in terms of miniaturization and portability, to provide a tool that can easily measure tissue oxygen metabolism in-vivo in a range of environments.

Developments in photonic devices have made this goal more realisable, with “mini”-bNIRS systems being created using adapted small volume spectrometers, to increase portability [4,5]. However, these solutions are still static systems restrained to testing labs, connected to the subject via long, and at times restricting, fibres. Recently, commercial spectrometers are moving away from the traditional Czerny-Turner design, by implementing focusing lenses and transmission gratings or by adopting Fastie-Ebert configurations, to miniaturise them further. This investigation considers three of these new generation miniature spectrometers, the C13054MA and the C14384MA by HAMAMATSU, which use lens-based designs and Fastie-Ebert configurations respectively, and the NSP32m N1 by NANOLAMBDA, which uses a plasmonic filer array and adaptive regularization. Compared to the most common spectrometer implemented in bNIRS systems, the QE65000 by Oceans Optics, which has dimensions of 182 mm x 110 mm x 40 mm, these alternative designs offer compactness with the C13054MA at 80 mm x 60 mm x 12 mm and the C14384MA at 11.5 mm x 4.0 mm x 3.1 mm and NSP32m at 34 mm x 9 mm x 5.5 mm. The purpose of this investigation is to determine the feasibility of these three spectrometers in a novel bNIRS device, by testing their response in the NIR range and assessing their SNR using a tissue-mimicking phantoms in comparison to two validated systems that provide the standard for oxCCO concentration change measurements.

Diffuse Optical Spectroscopy and Imaging IX, edited by Davide Contini, Yoko Hoshi, Thomas D. O'Sullivan, Proc. of SPIE Vol. 12628, 126282B
 · 0277-786X · doi: 10.1117/12.2668162

2. METHODS

A single channel was created across the surface of a tissue-mimicking phantom, using a custom 3D printed probe holder. At the source location, one end of an optical-fibre bundle that terminates with a 90° bend is inserted into the probe holder with the opposite end SMA connected to an Ocean Optics HL-2000-HP tungsten halogen lamp. This lamp emits in the wavelength range 360 to 2400 nm with a typical output power of 8.4 mW and is a common choice of light source for bNIRS systems[5,6]. The optical fibre has a bundle diameter of 1.4 mm with 30 µm core and NA of 0.57. At the other end of the probe holder, the spectrometers were set with the entrance slit against the phantom at a source-detector separation (SDS) of 2 cm, one at a time. The source remained switched on as spectra were acquired with the proprietary software, at integration times of 250 ms, 500 ms and 1000 ms. Then the source was switched off and dark noise acquisitions were made at each integration time. This was repeated for SDS of 2 cm, 3 cm and 4 cm. Phantoms based on the MEDPHOT protocol for standardized photon migration instrument testing, were used. The four phantoms are stable, cylindrical, homogenous solids, with specific optical properties labelled A2, B2, B3 and D7. Further descriptions of the phantom properties and constructions can be found in the original publication[7]. A, B, D correspond to the nominal scattering at 800nm of μ_s'= 5, 10, 20 cm^{-1} respectively and 2, 3, 7 correspond to absorption at 800 nm of μ_a'= 0.05, 0.10, 0.30 cm^{-1} respectively. A2 and D7 were chosen to simulate tissue with the least and most light interactions, and B2 and B3 are the phantoms with optical properties closest to brain tissue. For the HAMAMATSU detectors the acquisitions were taken in 16-bit A/D count against wavelength which was then used to determine the SNR of each detector in this set up, by comparison to the A/D counts in the dark periods. The NANOLAMBDA spectra were captured through an Arduino program used to control the device, and signal values are given in arbitrary units. All data processing was done in MATLAB version R2022a.

3. RESULTS

3.1 C13054MA

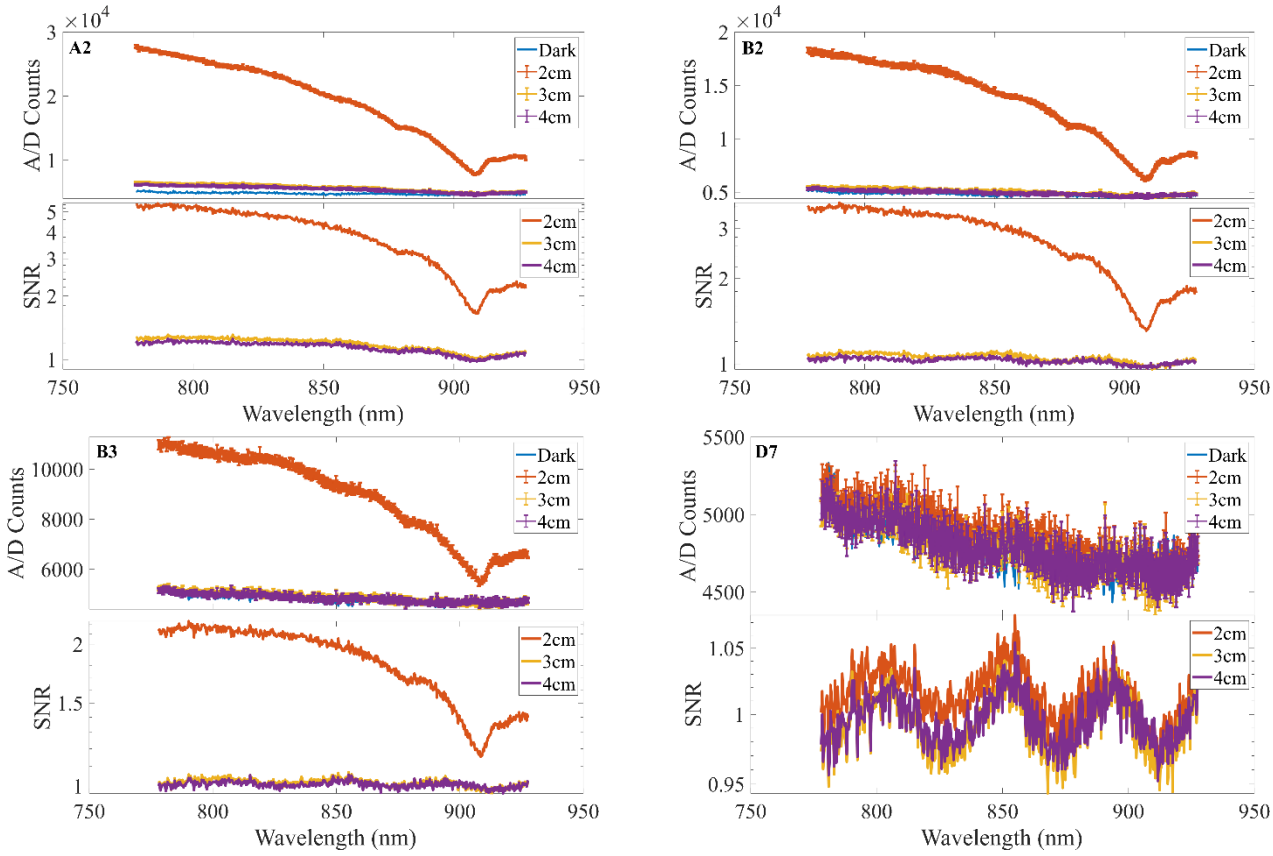

Figure 1: Spectra received through phantoms A2, B2, B3 and D7 at varied SDS with 250 ms integration time, averaged over 5 acquisitions for spectrometer C13054MA. SNR plotted below each spectra for each SDS at the same integration times.

The largest of the spectrometers, C13054MA is documented with a response range of 790 to 920 nm and a typical spectral resolution of 0.4 nm. The device in this investigation output counts at wavelengths steps of 0.29 nm on average. At integration times of 250 ms, as seen in Figure 1, the detectors are not saturated in any regime. For the low absorption phantom A2, 2 cm SDS maintains an SNR above 2 until after 900 nm, where it briefly drops below. 3 and 4 cm SDS give very similar intensity signals, with SNRs above 1 until >900 nm. For phantom B2 the SNR decreases across all separations, as expected, with 2 cm SDS dropping below SNR value 2 around 890 nm and remaining there until 920 nm. The signals from 3 and 4 cm separations are entirely dominated by noise, maintaining an SNR of 1 with slight fluctuations for all wavelengths, for all phantoms after this the 3 and 4 cm intensities remain dominated by noise. The final recoverable signal is for 2 cm SDS in phantom B3, where it drops below SNR values of 2 at 850 nm but does not reach 1. All signals can be considered unrecoverable in phantom D7.

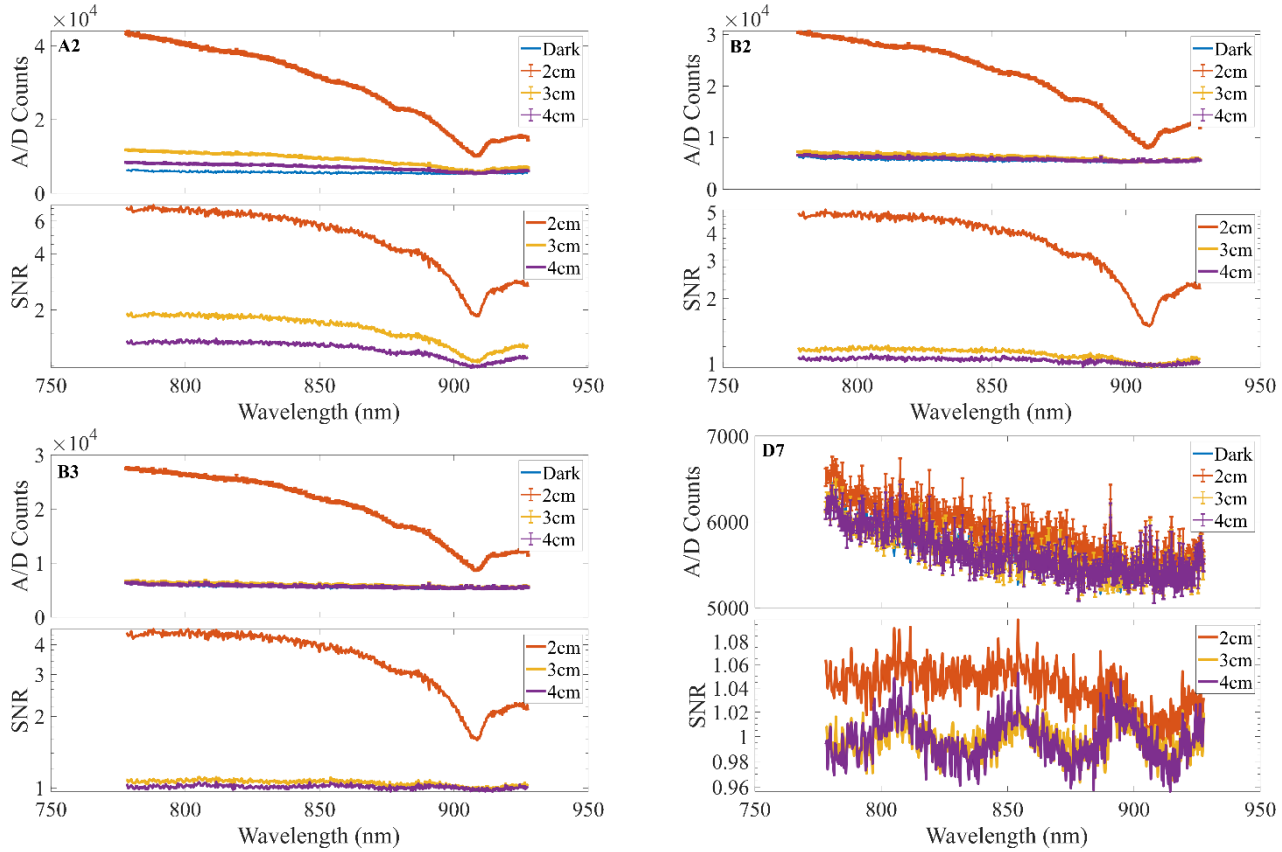

Figure 2: Spectra received through phantoms A2, B2, B3 and D7 at varied SDS with 500 ms integration time, averaged over 5 acquisitions for spectrometer C13054MA. SNR plotted below each spectra for each SDS at the same integration times.

Figure 2 outlines the spectra and SNR for 500 ms integration time, similarly to 250 ms there are no points of detector saturation across the 12 arrangements. In phantom A2, the SNR was between 6 and 2 for 2 cm separations but stayed below 2 for 3 and 4 cm. As with 250 ms integration times, the SNR for 3 and 4 cm SDS had dropped to 1 by phantom B3, with 2 cm SDS steadily decreasing in SNR at B2 and B3. Once again phantom D7 is too attenuating for any light detection at all detector separations.

At 1s integration times, the detector was saturated between 790 and 840 nm for SDS of 2 cm on phantom A2 shown in Figure 3, so no usable signal is recoverable in this range. Although the 2 cm separation is saturated, the SNR does not increase above ~8, giving us the upper limit on SNR for this detector at 1000 ms. For the other phantoms, the 2 cm separations result in higher SNR than previous integration times but the 3 and 4 cm separations have little to no appreciable difference from the 500 ms integration time. In the most optically dense phantom D7, there is some discernable signal for the 2 cm SDS, but of very low SNR.

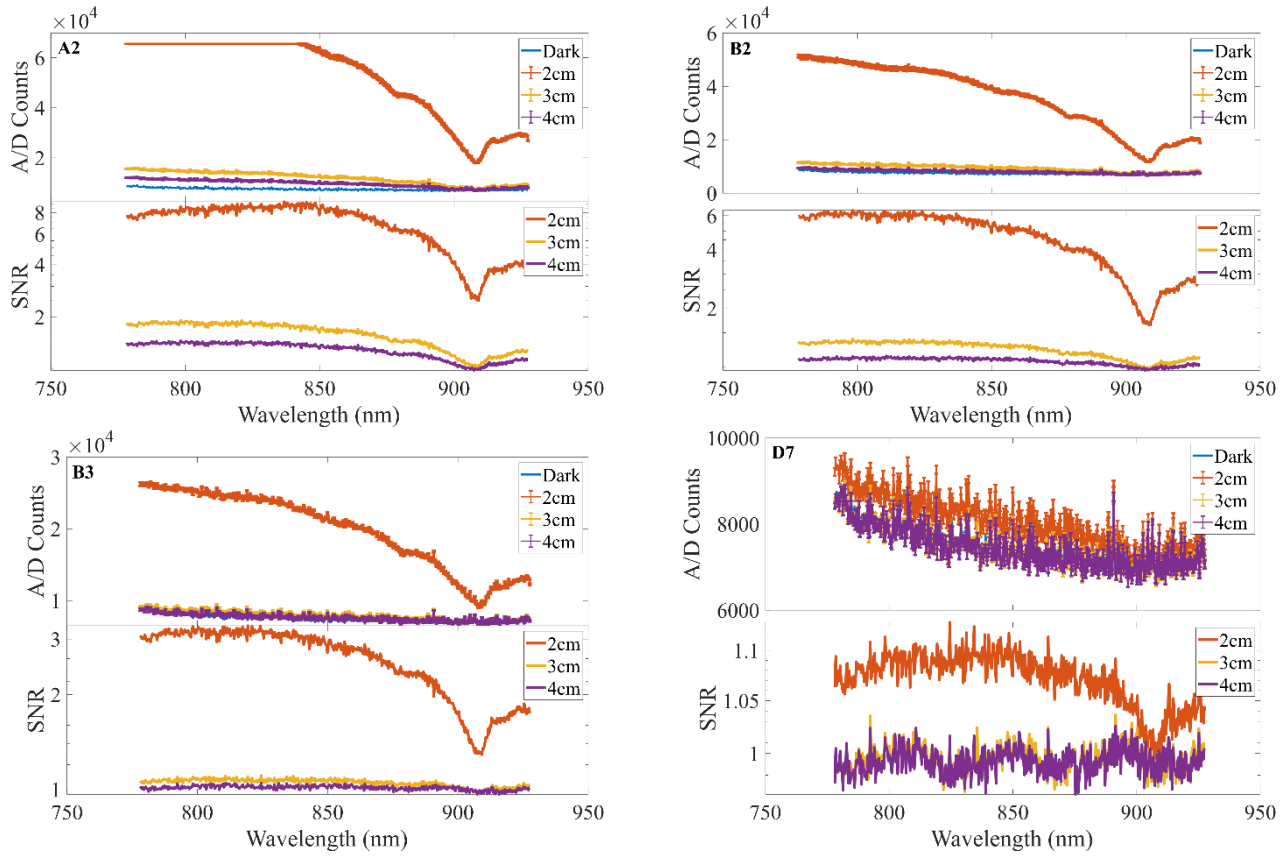

Figure 3: Spectra received through phantoms A2, B2, B3 and D7 at varied SDS with 1000 ms integration time, averaged over 5 acquisitions for spectrometer C13054MA. SNR plotted below each spectra for each SDS at the same integration times.

3.2 C14384MA

The surface mounted series device, C14384MA, has a documented spectral response of 640 to 1050 nm and a typical output resolution of 14 nm, however, the signal appears to begin with measurements at ~480 nm. The device also output counts per wavelength in a largely varied step size, ranging from 1.4 nm to 4.8nm, with an average of 2.7 nm sized steps. This investigation will only consider the documented response range for spectral analysis and SNR.

This high sensitivity micro spectrometer exhibited saturation even at the shortest integration time of 250 ms. The 2 cm SDS caused saturation from 640 nm to 970 nm in the A2 phantom, 640 nm to 960 nm in B2 and 655 nm to 915 nm in B3. In phantom D7 it was below saturation, with peak SNR of 8.7 at 818 nm and minimum of 1.2 at 1050 nm. For 3 cm and 4 cm SDS, in the first three phantoms, all wavelengths had SNR values above 1, in D7 these fell to 1.

As anticipated, increasing the integration times means that the 2 cm SDS configurations will remain saturated for all phantoms, with D7 being the exception again. Still, there is not enough light throughput to increase the SNR of 3 cm and 4 cm detection above a ratio of 1 for the D7 phantom, and in B3, 4 cm falls to SNR = 1 at 970 nm. For all other separations and phantoms, the SNR remains above 1 for the entire 640 – 1050 nm range.

In the final integration time of 1000 ms, SDS 2 cm causes saturation for the entire spectral range again, except in D7 where it maintains a high SNR. At these high integration times, the 3 cm separation also saturates in the A2 phantom, between 700 and 800 nm, and exhibits typical behaviors with SNR > 1 in B2 and B3, before being dominated by noise in D7 once more. 4 cm separations lead to SNR > 1 for all phantoms also, apart from D7.

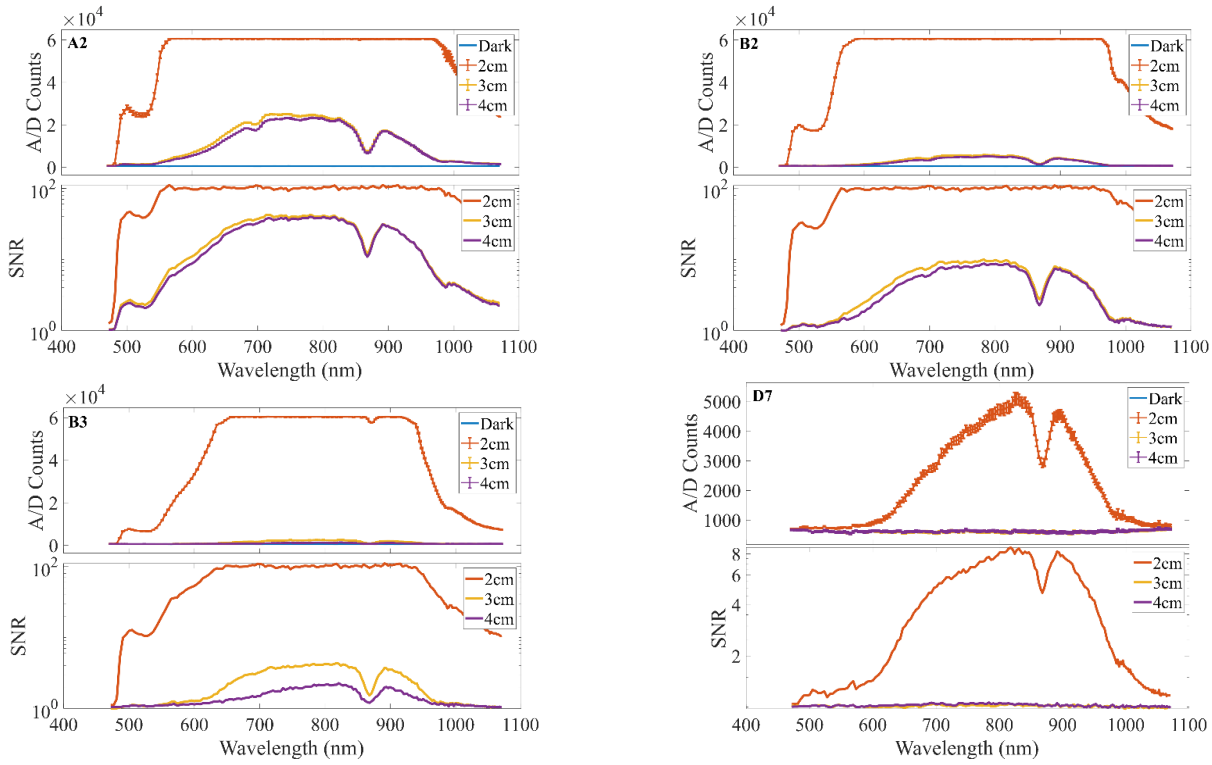

Figure 4: Spectra received through phantoms A2, B2, B3 and D7 at varied SDS with 250 ms integration time, averaged over 5 acquisitions for spectrometer C14384MA. SNR plotted below each spectra for each SDS at the same integration times.

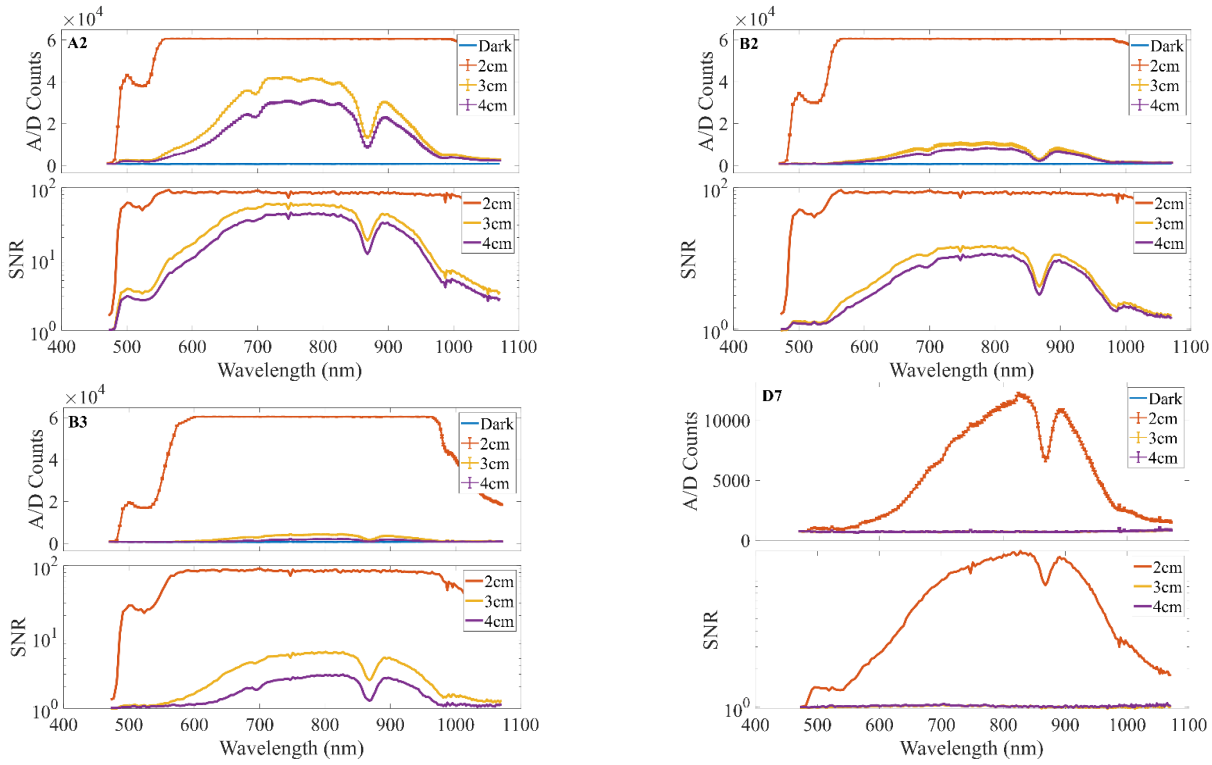

Figure 5: Spectra received through phantoms A2, B2, B3 and D7 at varied SDS with 500 ms integration time, averaged over 5 acquisitions for spectrometer C14384MA. SNR plotted below each spectra for each SDS at the same integration times.

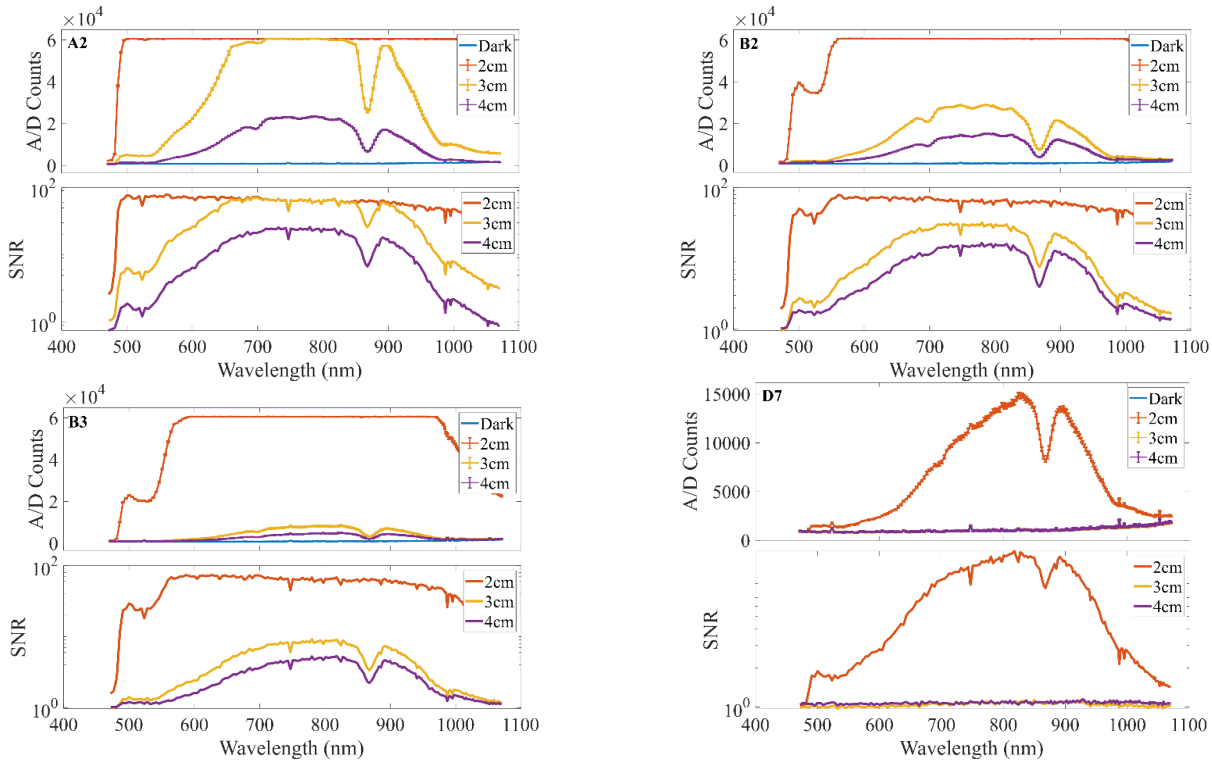

Figure 6: Spectra received through phantoms A2, B2, B3 and D7 at varied SDS with 1000 ms integration time, averaged over 5 acquisitions for spectrometer C14384MA. SNR plotted below each spectra for each SDS at the same integration times.

3.3 NSP32m N1

The smallest of the spectrometers in this test, the NSP32m N1 is documented with a response range of 600 – 1100 nm and a resolution of 25 – 30 nm. The step size for wavelength intensity measurements is an even 5 nm with no wavelength dependance. Due to the filter array and adaptive regularization techniques used in this device, saturation does not appear the way it does in the CMOS sensor spectrometer. Instead of flat lines at the count maximum, the device sends a saturation flag when any of its pixels are above the saturation limit. In this investigation, all saturated spectra were discarded in SNR calculations, as they had abnormal values. The wider FWHM wavelength resolution results in large gaps in the intensity per wavelength, leading to a discontinuous SNR graph where noise fell to zero, giving infinite SNR, where signal fell to zero, giving negatively infinite SNR, or where both signal and noise fell to zero.

With 2 cm SDS, the three phantoms A2, B2 and B3 are not optically attenuating enough to prevent saturation at all integration times. When used on the D7 phantom, they consistently exhibit SNR > 1 at each integration time, reaching as high as a SNR of 100 when using 1000 ms integration times. For 500 ms and 1000 ms, the sensor was saturated when applied to the A2 phantom at any SDS. At 1000 ms, the 3 cm separation is close enough to saturate the sensor on the B2 phantom.

Where the sensor does not saturate, the SNR is consistently above 1 for the measured signals in phantoms A2, B2 and B3. In D7, the SNR values for 3 and 4 cm SDS fluctuate around 1 and are largely dominated by the noise. There are also points where the signal drops below the dark signal, which is likely a result of the adaptive regularization algorithm in very low light settings.

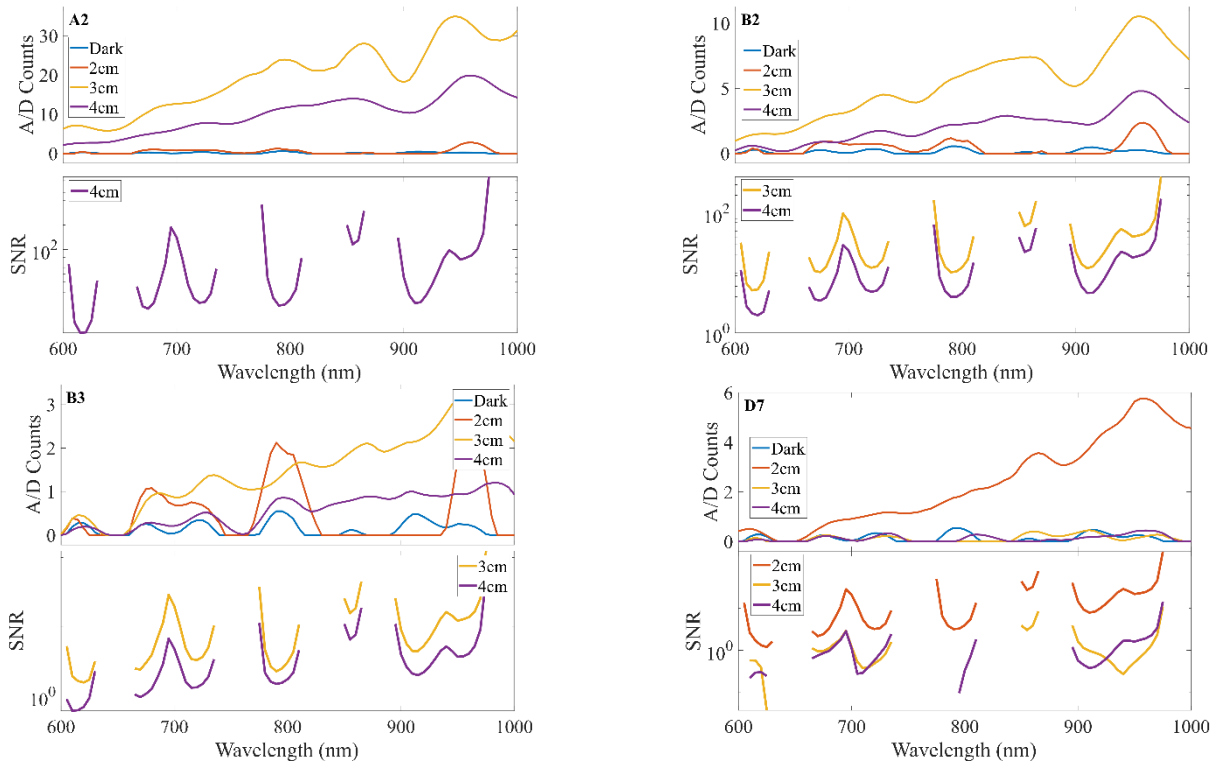

Figure 7: Spectra received through phantoms A2, B2, B3 and D7 at varied SDS with 250 ms integration time, averaged over 5 acquisitions for spectrometer NSP32m N1. SNR plotted below each spectra for each SDS at the same integration times.

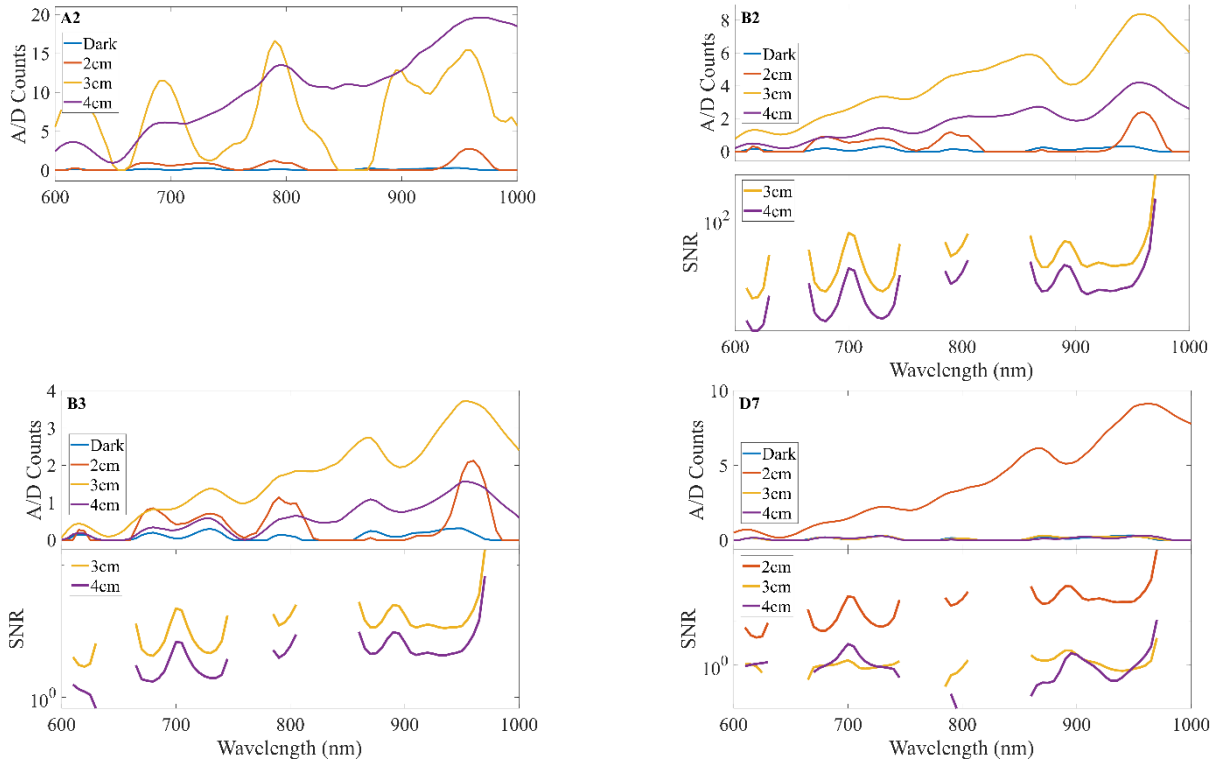

Figure 8: Spectra received through phantoms A2, B2, B3 and D7 at varied SDS with 500 ms integration time, averaged over 5 acquisitions for spectrometer NSP32m N1. SNR plotted below each spectra for each SDS at the same integration times.

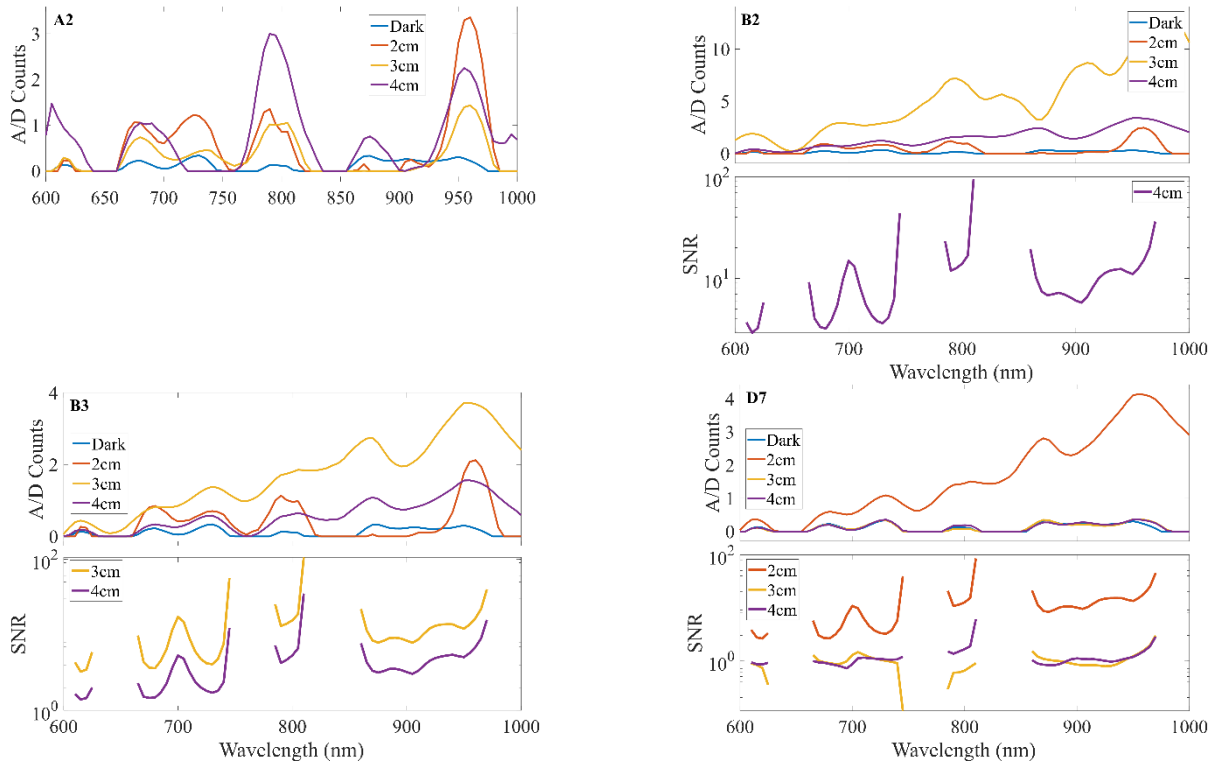

Figure 9: Spectra received through phantoms A2, B2, B3 and D7 at varied SDS with 1000 ms integration time, averaged over 5 acquisitions for spectrometer NSP32m N1. SNR plotted below each spectra for each SDS at the same integration times.

3.4 Comparison to current bNIRS systems

Two gold-standard bNIRS systems, used to determine changes in oxCCO in vivo, are used to benchmark these novel spectrometers. Each of these systems uses a spectrometer and white light source; the CYRIL system uses a benchtop spectrometer with thermoelectric cooling to -70˚C and has 8 channels each connected to the spectrometer by a vertically arranged fibre bundle[8]. The mini-CYRIL makes use of a smaller, portable spectrometer and provides a single channel with tungsten halogen lamp source[5]. The comparison is made with the B2 phantom, as it is closest to optical properties encountered when making cerebral measurements, at 500 ms and 1000 ms and a SDS separation of 3 cm, typically used to reach depths required to make cerebral oxygenation and metabolism measurements.

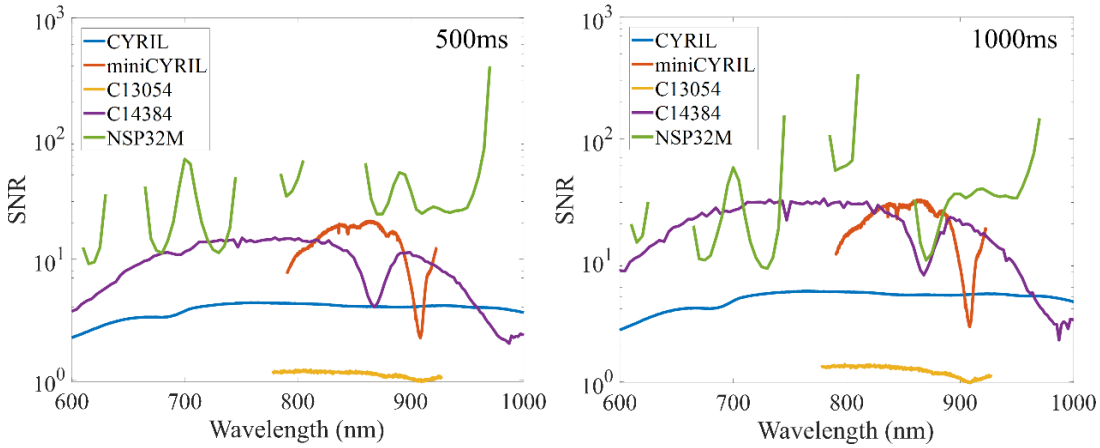

Figure 10: Comparisons of the SNR for 5 different spectrometers in typical bNIRS cerebral measurement configurations; phantom B2, SDS 3cm and taken at integration times 500 ms and 1000 ms

Of the novel spectrometers in this set up, the NSP32M performs the best for SNR, with values between 10 and 100 for both 500 and 1000 ms integration times, even reaching beyond 100 at times. The discontinuities in the SNR plot are from positive infinite values, where the recorded dark count at those wavelengths was zero, however this can also appear where the signal is also zero due to the large spacing in wavelength resolution. In all wavelength ranges shared with CYRIL and miniCYRIL, it outperforms them in a 1:1 comparison of SNR.

The surface mounted C14384MA reaches SNR of 10 at its peak in 500 ms integration times, which surpasses the CYRIL system, however it is close to, but behind, the SNR of miniCYRIL. This changes when using 1000 ms integration times, where the micro-spectrometer appears it would surpass the miniCYRIL SNR if not for a large attenuation spike, regardless it continues to outperform the CYRIL spectrometer. The C14384MA also covers a wider range of wavelengths than the miniCYRIL and the other micro-spectrometers.

The C13054MA under performs here, with considerably low SNR, near 1, for both integration times. Though it has strength in the very fine resolution of 0.4 nm, the signals received at the spectrometer are extremely low and hard to distinguish from the dark noise.

4. DISCUSSION

This study explores the feasibility of three novel miniature spectrometers as detectors for bNIRS systems. In the case of the C14384 and the NSP32M, the 2 cm SDS was over saturated at all integration times in cerebral mimicking phantoms. At times, short channel separations are used to improve the contrast of fNIRS measurements[9], which would not be possible for these spectrometers at any integration time greater than 250 ms. It is possible to implement an optical density in the 2 cm SDS channel to allow for resolving of all SDS at these integration times.

The study was conducted with a commonly used quartz-tungsten halogen lamp as the light source; if bNIRS is to become wearable then bulky and heavy lamps cannot be used freely. Broadband LEDs provide a white light source suitable for bNIRS, but at a much lower power output, which will affect the SNR and integration times may need to be adjusted to compensate.

The software implementation of these spectrometers is no more complicated than regularly used alternatives; custom device housings may be required to use the spectrometer slit-to-skin approach. The C13054MA offers SMA connectors, which can allow for a more flexible optical fibre connection, allowing the spectrometer to be set away from the body, and could improve SNR by increasing light collection efficiency. The investigation was also conducted in a dark, temperature-controlled room to isolate dark noise and test sensitivity. More work will be done to determine reproducibility in realistic implementations and determine heating effects on each novel device.

To conclude, there is evidence that the new generation of miniature spectrometers are suitable for use in bNIRS measurements. Future testing, when paired with miniaturized light sources, will determine if these can be used to create a new wearable and portable device for non-invasive hemodynamic and metabolic monitoring.

ACKNOWLEDGEMENTS

FL was supported by Wellcome Leap Fund Inc (US) PROSPEKT, Study Award Number 185284. FL and IT are supported by UCL, which, as UK participant in Horizon Europe Project HyperProbe, is supported by UKRI grant number 10048387.

REFERENCES

[1] K. L. Perdue, S. K. Jensen, S. Kumar, J. E. Richards, S. H. Kakon, R. Haque, W. A. Petri, S. Lloyd-Fox, C. Elwell, and C. A. Nelson, “Using functional near-infrared spectroscopy to assess social information processing in poor urban Bangladeshi infants and toddlers,” Developmental Science, vol. 22, p. e12839, 9 2019.

[2] G. Bale, S. Mitra, and I. Tachtsidis, “Metabolic brain measurements in the newborn: Advances in optical technologies,” Physiological Reports, vol. 8, 9 2020.

[3] C. E. Cooper and R. Springett, “Measurement of cytochrome oxidase and mitochondrial energetics by near-infrared spectroscopy.,” Philosophical Transactions of the Royal Society B: Biological Sciences, vol. 352, no. 1354, p. 669, 1997.

[4] M. Diop, E. Wright, V. Toronov, T.-Y. Lee, and K. S. Lawrence, “Improved light collection and wavelet de-noising enable quantification of cerebral blood flow and oxygen metabolism by a low-cost, off-the-shelf spectrometer,” vol. 19, p. 057007, 5 2014.
[5] P. Kaynezhad, S. Mitra, G. Bale, C. Bauer, I. Lingam, C. Meehan, A. Avdic-Belltheus, K. A. Martinello, A. Bainbridge, N. J. Robertson, and I. Tachtsidis, “Quantification of the severity of hypoxic-ischemic brain injury in a neonatal preclinical model using measurements of cytochrome-c-oxidase from a miniature broadband-near-infrared spectroscopy system,” vol. 6, p. 045009, 11 2019.
[6] M. Diop, E. Wright, V. Toronov, T.-Y. Lee, and K. S. Lawrence, “Improved light collection and wavelet de-noising enable quantification of cerebral blood flow and oxygen metabolism by a low-cost, off-the-shelf spectrometer,” vol. 19, p. 057007, 5 2014.
[7] Pifferi, A., Torricelli, A., Bassi, A., Taroni, P., Cubeddu, R., Wabnitz, H., Grosenick, D., Möller, M., Macdonald, R., et al., “Performance Assessment of Photon Migration Instruments: The MEDPHOT protocol,” Applied Optics 44(11), 2104 (2005).
[8] Bale, G., Mitra, S., Meek, J., Robertson, N., and Tachtsidis, I., “A new broadband near-infrared spectroscopy system for in-vivo measurements of cerebral cytochrome-c-oxidase changes in neonatal brain injury,” Biomedical Optics Express 5(10), 3450 (2014).
[9] Goodwin, J. R., Gaudet, C. R., & Berger, A. J. “Short-channel functional near-infrared spectroscopy regressions improve when source-detector separation is reduced.” Neurophotonics, 1(1), 015002. (2014).